A QUANTITATIVE MODEL OF INTERSARCOMERE DYNAMICS DURING FIXED-END CONTRACTIONS OF SINGLE FROG MUSCLE FIBERS

D. L. MORGAN, S. MOCHON, AND F. J. JULIAN
Department of Muscle Research, Boston Biomedical Research Institute, 20 Staniford Street, Boston, Massachusetts 02114

ABSTRACT A numerical model of a muscle fiber as 400 sarcomeres, identical except for their initial lengths, was used to simulate fixed-end tetanic contractions of frog single fibers at sarcomere lengths above the optimum. The sarcomeres were represented by a lumped model, constructed from the passive and active sarcomere length-tension curves, the force-velocity curve, and the observed active elasticity of a single frog muscle fiber. An intersarcomere force was included to prevent large disparities in lengths of neighboring sarcomeres. The model duplicated the fast rise, slow creep rise, peak, and slow decline of tension seen in tetanic contractions of stretched living fibers. Decreasing the initial non-uniformity of sarcomere length reduced the rate of rise of tension during the creep phase, but did not decrease the peak tension reached. Limitations of the model, and other processes that might contribute to the shape of the fixed end tetanic tension record are discussed. Taking account of model and experimental results, it is concluded that the distinctive features of the tension records of fixed end tetanic contraction at lengths beyond optimum can be explained by internal motion within the fiber.

INTRODUCTION

In a previous publication, (Julian and Morgan, 1979 *a*) evidence was presented that during tetanic contractions at lengths longer than the optimum for tension generation, frog single fibers showed internal motion, as had been reported before by Huxley and Peachey (1961), Gordon et al. (1966 *a*), and Julian et al. (1978 *b*). The existence of this motion, the resulting slow creep phase of tension rise, and the effects of varying degrees of non-uniformity were qualitatively explained in terms of instability of sarcomere lengths due to the characteristic decrease of tension generating capacity with increasing sarcomere length in this region. This explanation of the creep phase of tension rise was used by Gordon et al. (1966 *a*) to justify their method of measuring the sarcomere length-tension diagram, which provides important support for the cross-bridge theory of muscle contraction.

If the slow phase of tension rise is due to internal motion, then the Gordon et al. curve is fundamental. If the non-uniformity explanation is wrong and the slow rise is an inherent part of activation at these lengths, then more complex relationships (e.g., Ramsey and Street, 1940, or Edman, 1966) must be considered fundamental. The present work aims to provide a more quantitative version of the internal motion explanations, which have been criticized by ter Keurs et al. (1978), by constructing a numerical model of a fiber as a series of simple "sarcomeres," identical except for their initial sarcomere lengths. A mechanical equivalent of three sarcomeres is drawn in Fig. 1 *A*, which shows that the sarcomere model is basically phenomenological, not structural, in that it makes no attempt to model muscle in terms of cross-bridge dynamics. Such an approach would be preferable, but exceedingly complex. Instead, the basic properties of muscle are modelled mathematically, similarly to the approach of Hill (1938), but recognizing that the parameters vary with sarcomere length, and applying the lumped model to represent a sarcomere instead of a whole muscle. These sarcomere models are then connected in series to simulate a fiber.

METHODS

The model involves a number of assumptions about a muscle fiber, some of which are simplified. The main assumptions and some of their limitations are listed here.

(*a*) All sarcomeres in a fiber have identical properties. The cross-sectional area of a muscle fiber varies somewhat along its length (Blinks, 1965), suggesting that the tension capability may also vary somewhat. The passive force-length characteristic can be expected to vary more significantly, due to occasional attached strands of connective tissue. At the ends, in particular, microscopic examination reveals that a fiber tapers, has tendinous strands inserting at different points, and has nonuniform passive sarcomere lengths (Huxley and Peachey, 1961), suggesting different passive properties. An example is Fig. 1 *B* of Julian et al. (1978 *a*). The assumption is justified if all these variations are small compared with the variation of active tension with sarcomere length.

(*b*) Each sarcomere has a uniquely defined sarcomere length. This is equivalent to assuming that the striations stay straight and perpendicular to the axis of the fiber. Examination of fiber photographs shows that

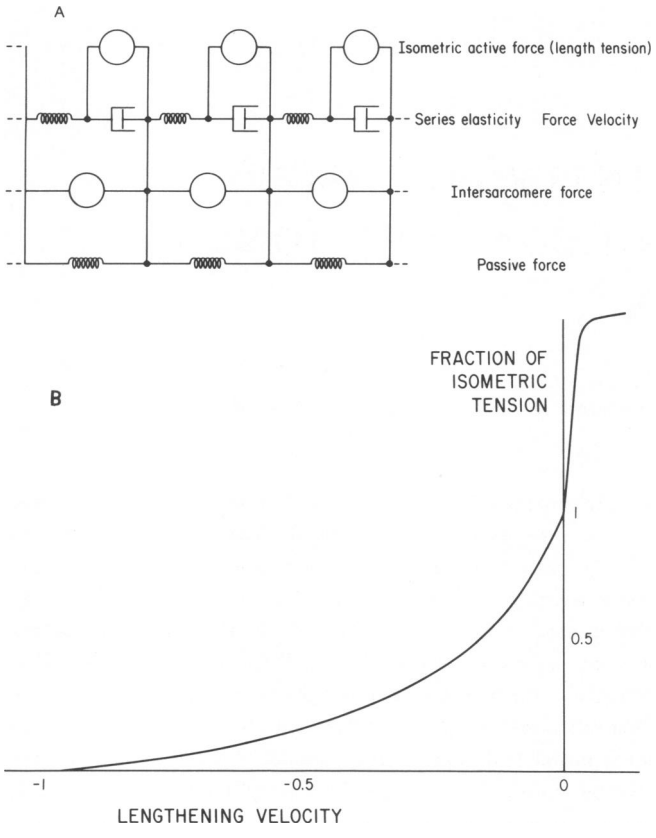

FIGURE 1 *A*, mechanical representation of a three sarcomere segment of the "fiber." The total sarcomere force has three components independent of length change and one dependent. Isometric force P_o is determined from the length according to the Gordon et al. (1966 *b*) relationship. Intersarcomere force is determined from the length of this sarcomere and its neighbors. Passive force is determined from length according to Fig. 7 of Edman (1979). The fourth component represents the force velocity curve, and is represented mechanically by a viscous element with damping coefficient equal to the chord slope of the appropriate force-velocity diagram, i.e., a function of length, isometric tension and velocity. The length change is the sum of length changes in the damper and the series elasticity. *B*, force-velocity curve. The formulae are $V/V_{max} = (-5/16)/(P/P_o + 1/4) + 1/4$ for shortening; and $V/V_{max} = 0.8 \times 0.002/1.8 - P/P_o - 0.002 + P/P_o - 1/32.43$ for lengthening. The lengtheing velocity is in units of μm/sarcomere/time unit.

this is often not the case, particularly at long fiber lengths. The observation that this skewing and distortion are more noticable during a tetanus than in a passive muscle, particularly at long length, suggests that they may well be significant. The inclusion of such phenomena would, however, have greatly increased the complexity of the model.

Implicit in this assumption also is the equality of the two halves of a given sarcomere; i.e., no provision has been made for misalignment of thick filaments within a sarcomere. This was also omitted for simplicity and may be a significant limitation of the model.

(*c*) The isometric tension varies with sarcomere length according to the idealized curve of Gordon et al. (1966 *b*, Fig. 12); that is, force is maximal between sarcomere lengths 2.0 and 2.25 μm, decreasing linearly beyond 2.25 to 0 at 3.65 μm. Below 2.0 μm, tension decreases to 84% maximal at 1.67 μm, and then more steeply to zero at 1.27 μm.

(*d*) The tension varies with steady velocity, as shown in Fig. 1 *B*. For shortening, a hyperbola is used where (in Hill's [1938] terminology) $b/V_{max} = a/P_o = 0.25$. For lengthening, another hyperbola is used, with 1.8 P_o (Katz, 1939) as one asymptote, and a straight line through the isometric point, with a slope equal to six times the slope of the shortening hyperbola at very small shortening velocities as the other (Katz, 1939). The unloaded shortening velocity, V_{max}, was assumed constant for sarcomere lengths >1.85 μm, linearly decreasing to zero at 1.3 μm (Gordon et al., 1966 *b*, Fig. 11). This is an approximation, but varying it, even to being constant at all lengths, did not change the results significantly.

(*e*) Passive force is purely elastic, and it is the same for each sarcomere. As noted in assumption (*a*) above, passive stiffness probably varies along a fiber, but apart from determining initial sarcomere spacings, these variations are probably not important. The viscoelastic nature of passive force is important. For example, Gordon et al. (1966 *a*, p. 167) found that the passive resistance to stretch at very long lengths at the velocities observed during creep was five times greater than the static stiffness. Consequently, the model will be seriously in error at sarcomere lengths where passive tension is significant, i.e., beyond ~3.0 μm sarcomere length. This error will be in the conservative direction, underestimating the force due to internal motion. Including nonelastic passive behavior would require introducing a second velocity-dependent element into the sarcomere model, considerably increasing the computation complexity.

(*f*) A series compliance such that a shortening of 12 nm/one-half sarcomere would drop the force from isometric to zero is included in each model sarcomere. Without some series compliance, the tension would change to the new steady-state value as soon as velocity changed. For example, a ramp of muscle length such as was used to generate the records in Fig. 2 would result in a square wave of force, with no smoothing. Also, any shortening faster than V_{max}, no matter how small, would reduce the tension to zero. This compliance was made inversely proportional to isometric tension in view of the finding that the stiffness of a carefully mounted single fiber is proportional to force with varying overlap, and hence principally due to the cross-bridges (Huxley and Simmons, 1971). The value of shortening needed to drop the force to zero corresponds to the T_2 intercept of Ford et al. (1977), as the present model does not represent the fast tension transients first recorded by Huxley and Simmons (1970).

(*g*) Activation reaches maximum value instantaneously at the beginning of a tetanus. Provided that the time actually taken is uniform along the fiber, and small compared to the creep time, this simplification should not seriously affect the results, other then rounding the initial rise, as seen in Fig. 4.

(*h*) A short sarcomere acts to shorten its neighbor, and a long sarcomere to lengthen its neighbor. This assumption is necessary to explain certain features of the behavior of fibers microscopically observed during contractions at long length. The regions of shortened sarcomeres at the ends are seen to merge gradually into the rest of the fiber; i.e., sharp divisions between populations of sarcomeres with different lengths are not seen. Also, it is possible to observe this shortened region incorporating neighboring longer sarcomeres. Correspondingly, Julian and Morgan (1979 *a*) showed that the length of the central part of a fiber, measured using markers and the spot follower apparatus, continues to increase throughout a long tetanus. From these observations it is concluded that some force or process must act against one sarcomere being much shorter than its neighbor.

Probably the most obvious way in which such a force could be generated in a real muscle fiber arises from the constant volume behavior of a fiber. A shorter sarcomere would be wider, but the fiber structures, including the sarcolemma, are continuous between sarcomeres and would resist sudden changes of fiber diameter, and hence sarcomere length. Another possible mechanism is suggested by Peachey and Eisenberg's (1978) observation of helical structure in a fiber. A short patch in one sarcomere would spread across that sarcomere, each myofibril shortening its neighbor until the neighbor was short enough and consequently strong enough to shorten itself. This spreading across a sarcomere could continue around the helix and appear in the "next" sarcomere; that is, the helical structure could convert the spreading across the fiber into spreading along the fiber. There is no direct evidence that the helical structure is involved in this process, but it is an interesting possibility.

In the model each sarcomere was subjected to passive forces, propor-

tional to the difference in length between it and its neighbor on each side, acting to lengthen it if the neighbor was longer, and shorten it if the neighbor was shorter. Thus no extra active force is generated, but force generated in one sarcomere is transferred to another. The effect of removing the intersarcomere force is shown in Fig. 5.

CALCULATION PROCEDURE

Only one-half of a fiber was represented; i.e., only one end with shorter sarcomeres was included. For each discrete time interval, the program calculated the passive forces and isometric tetanic force capability of each of 200 sarcomeres, using the sarcomere lengths found at the end of the last time interval. An estimate of total fiber force was then made, and for each sarcomere, the required active force was found. Using the force-velocity relationship for each sarcomere, the length change that would result in one time interval, if the postulated force acted, was calculated. These length changes were then summed, giving the total length change of the fiber. If this was not equal (within a specified accuracy) to the desired movement in that time interval (zero for fixed end conditions), a new estimate was made of the force, and the process iterated until this condition was met. When it was, the sarcomere lengths were updated, by adding the length changes to the previous lengths, and the next time interval considered. The number of sarcomeres in the model is still an order of magnitude less than in a real iliofibularis fiber, in the interests of computational speed. If the number was reduced by another order of magnitude, the records become "lumpy" as individual sarcomeres passed through the optimum length range.

The time intervals were 0.05 time units, where a time unit was defined as the reciprocal of the unloaded shortening velocity (at 1.85 μm or longer) expressed in μm/sarcomere/s. The passive tension was given by an exponential curve fitted to the curve published by Edman (1979, Fig. 6). $\ln P = 6.05\,l - 21$ where P is the passive tension in units of maximum

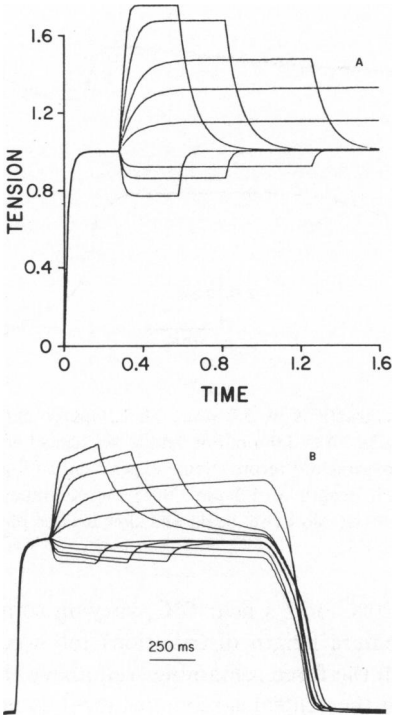

FIGURE 2 Stretches and releases at optimum length. *A*, Model, stretches and releases are at 0.5, 1.1, 1.8, 3.1, and 5.2 V_{max} in each case, between sarcomere lengths of 2.04 and 2.21 μm. *B*, Fiber, the experimental records are from a single *Rana temporaria* anterior tibialis fiber at 18°C, using velocities to match those in *A*.

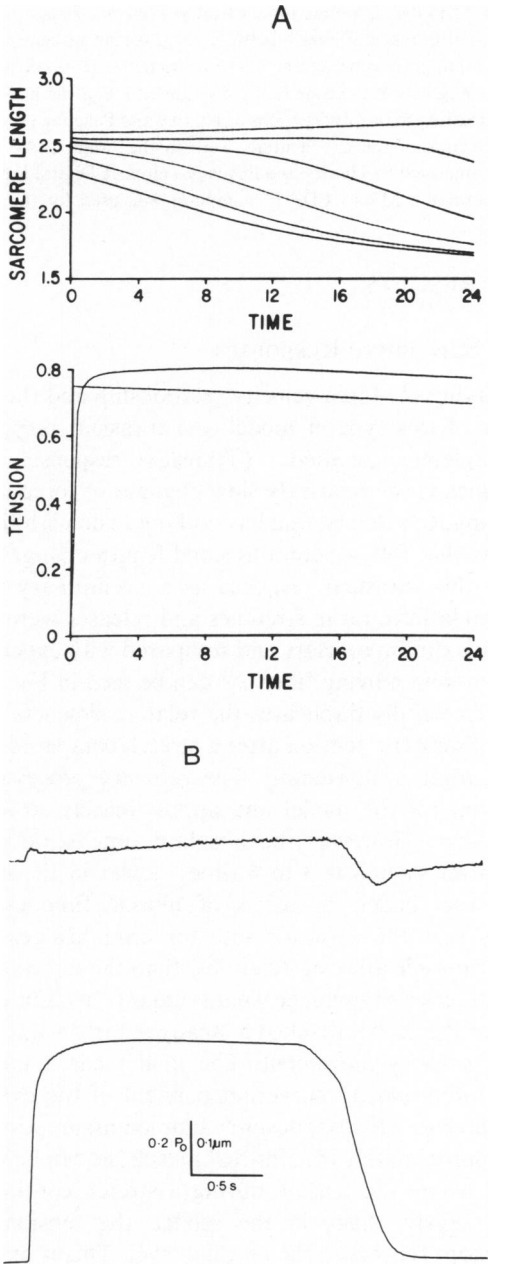

FIGURE 3 Contractions at 2.6 μm. *A*, computer output for fixed end simulation. The time unit is the reciprocal of V_{max} in μm/sarcomere/s, hence 1 s is ~18 time units at 20°C, 8 at 10°C, or 4 at 0°C. In the tension panel, the upper line is the tension generated in units of P_o, the lower is the isometric capability of the central sarcomeres. There were 200 sarcomeres in the model of half a fiber. Sarcomere lengths are shown in micrometers for sarcomeres number 1 (lowest), 6, 11, 16, 21, and 200 (longest). Initial sarcomere lengths 2.3 to 2.6 μm. Note the continuous lengthening of the sarcomeres in the centre of the fiber, as shown by 200, throughout the tetanus. *B*, a comparable experimental record. Single fiber from tibialis anterior of *Rana temporaria* during fixed end contraction at initial sarcomere length of 2.58 μm. Upper trace is the spot follower record, showing the length of a central segment of the fiber, calibrated as sarcomere length in micrometers. Lower trace is tension. Experiment 78/5-2.5. Temperature = 12°C. See Discussion section for comparison.

isometric tension, l is sarcomere length in microns, and ln is the natural logarithm. The intersarcomere force constant used was P_o per micrometer; that is, a difference of length between neighboring sarcomeres of 0.1 μm led to an intersarcomere force of 0.1 of isometric tension. The initial sarcomere lengths were exponentially distributed along the half fiber as an approximation to the observations of Huxley and Peachey (1961). The length constants of the exponentials were in the range 2–4% of fiber length, as suggested by Huxley and Peachey's plots. A Digital Equipment Corp. (Southboro, Mass.) PDP-11 computer was used for the calculations.

RESULTS

Sarcomere Responses

By specifying the force-velocity relationship and the series elasticity of this type of model, the transient response is also completely specified. (Transient response in this context means the relatively slow changes of force following a change in velocity, and has nothing to do with the fast transients that follow submillisecond length changes.) To examine this transient response as a preliminary to the creep simulations, ramp stretches and releases were simulated at maximum overlap, and compared with experimental results from a living fiber. As can be seen in Fig. 2, the model successfully duplicates the relative slowness of the return to isometric tension after a stretch compared to the recovery after a shortening. The recovery processes are exponential for the model and approximately so for the muscle fiber. However, the absolute time scale of the decline after stretch is 3 to 4 times slower in the muscle than in the model. In terms of muscle function, this indicates that the turnover rate for cross-bridges in an isometric muscle after stretch is less than the force-velocity curve and series compliance would suggest. In addition, the tension of the model reached a steady value during a long constant velocity movement. The model has a uniquely defined force-velocity curve independent of the extent of the movement, whereas, despite common assumption, this is only approximately true for real muscle, as can be seen in Fig. 2 *B* where the tension during a stretch continues to increase slowly. Also, in the model, the tension after motion stops returns to the original level. This is only true for muscle if considerable care is taken to confine sarcomere lengths to the plateau and to wait a long time for a final value to be reached. (Julian and Morgan, 1979 *b*, Fig. 4 *B*.) All these discrepancies are directed so as to reduce the tension seen during creep in the model relative to the real muscle. They are limitations of the model, and cannot be eliminated without disturbing the fit to other characteristics, or by using a much more complex model.

Creep Simulations

Two representative runs are shown in Fig. 3 *A* and 4 *A*, and the conditions and parameters are listed in the legend of Fig. 3. The tension is seen to have a rapid upstroke to near the level appropriate to the central sarcomeres, followed by a slow rise (creep) to a peak at ~10 time units

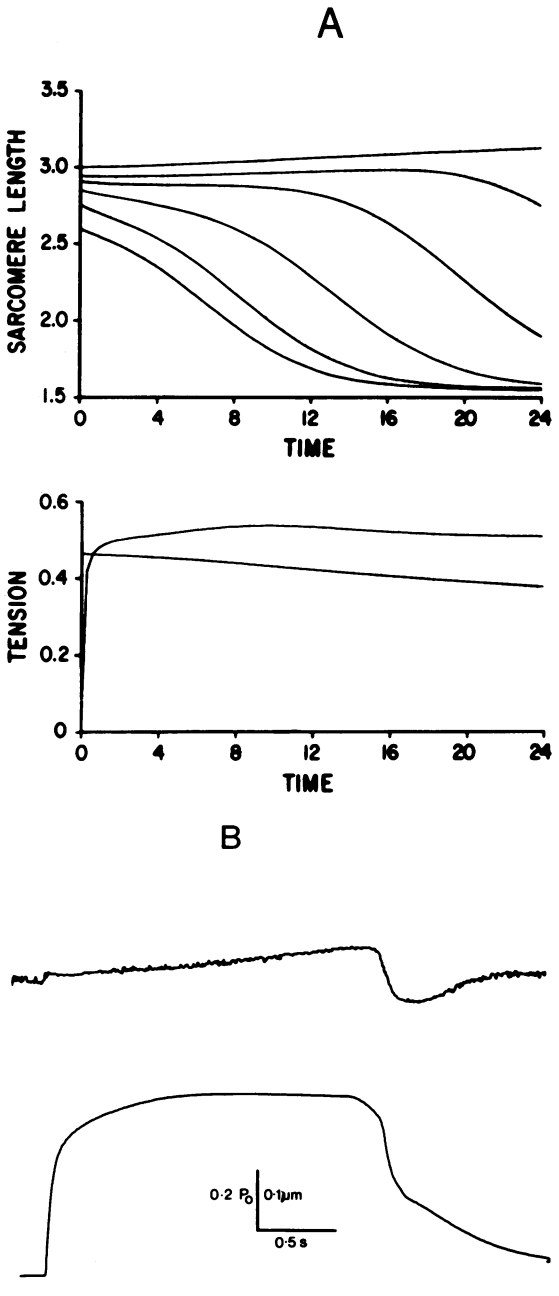

FIGURE 4 Contractions at 3.0 μm. *A*, computer output for initial sarcomere lengths 2.6 to 3.0 μm. For details, see legend of Fig. 3 *A*. *B*, a comparable experimental record. Same experiment as Fig. 3 *B* but with initial sarcomere length of 3.0 μm. Note the continual slow internal motion and fast rise, slow rise, peak, and slow decline phases of tension trace.

(~0.5 s at 20°C or 2 s near 0°C, varying somewhat with initial sarcomere length distribution) followed by a slow decline, with the force remaining well above the isometric capability of the central sarcomeres throughout the tetanus. This maintained extra tension is accompanied by a continued lengthening of most of the fiber. This lengthening is taken up by the active shortening of sarcomeres in the transition region between those sarcomeres that have shortened past optimum length and those that are still

lengthening. As each sarcomere shortens, the intersarcomere force acts to shorten its neighbor on the long side, until that neighboring sarcomere is sufficiently short to actively shorten itself. In this way, the transition zone is maintained, and there are always sarcomeres able to shorten, so lengthening the rest of the fiber, and maintaining the raised tension. After a long contraction, such as at the end of Fig. 3 *A*, there is an area of very short sarcomeres at the end of the fiber, a transition region of actively shortening sarcomeres of intermediate length (no "forbidden lengths"), and a large area of very slowly lengthening sarcomeres away from the end of the fiber. Increasing the duration of the contraction increases the number of shortened sarcomeres, but does not abolish the transition zone, or the shortening of sarcomeres within it. The intersarcomere force ensures that sarcomeres continuously pass from lengthening into the "long" end of the transition zone, to replace those that pass from the "short" end of the transition zone to the "shortened" zone, so that the transition zone slowly moves along the fiber. For any feasable duration of tetanus however, the shortened region is always a small portion of the total fiber length; e.g., <5% of the sarcomeres in the fiber at the end of the contraction shown in Fig. 3 *A*. The velocity of stretch of central sarcomeres did not exceed 1% V_{max}, which produces almost 29% active tension enhancement. The greater apparent enhancements seen in fibers at very long length, see Julian and Morgan 1979 *a*, Fig. 7 (3.4 μm) are easily explained by increased passive tension as a result of the stretch (Gordon et al., 1966 *b*). The total stretching of central sarcomeres up to the tension peak is <0.1 μm/sarcomere. It must be emphasized that this is a very slow speed, not easily detected by photography or laser diffraction, particularly in view of the uncertainties and artifacts illustrated by Rudel and Zite-Ferenczy (1979). For a further discussion on the use of laser diffraction in this context, see A.F. Huxley (1980, pp. 57–59). However, movement has been documented photographically by Julian et al. (1978 *b*) and using lasers by Haskell and Carlson (1981), ter Keurs et al. (1978) did not find it consistently, though some of their records do show stretching of a central segment, as in the lower panel of Fig. 6.

By using very short segments of skinned fibers it is possible to monitor closely all or most of the sarcomeres (see Fabiato and Fabiato [1978]) using cardiac rather than skeletal muscle. Under these conditions however, other difficulties arise. The damaged ends and attachments, though small, are a considerable portion of the segment. For segments >8 μm wide, they reported that the striation pattern was lost during contraction, whereas it remains visible in a 200-μm–wide whole skeletal fiber. Even for very thin segments such as their Fig. 1 *C* where sarcomeres are still visible, there is considerable skewing of sarcomeres, so that the length of a given sarcomere varies significantly across the muscle segment. Under these conditions, the assumption of a uniquely definable length for each sarcomere is not met, and the non-uniformities are much more complex than those considered in this model.

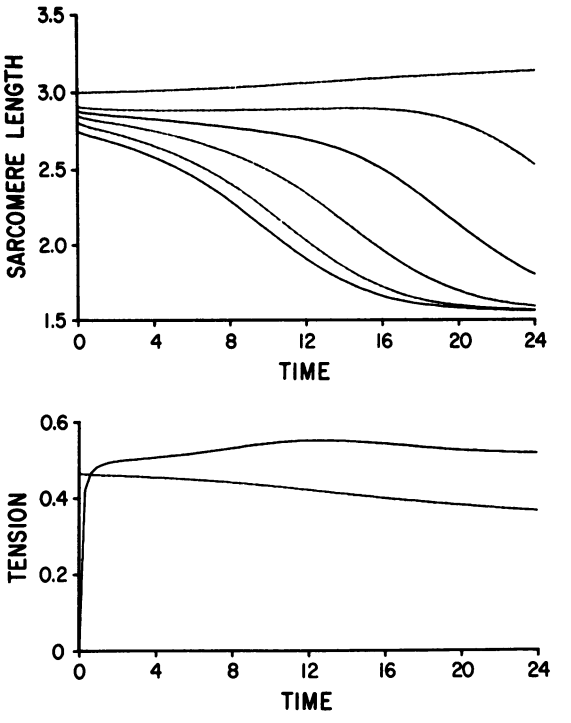

FIGURE 5 The effect of intersarcomere stiffness. The initial conditions were identical to Fig. 3 *A* except that the intersarcomere stiffness was removed. The peak tension is not significantly less, but the decline after the peak is greater.

Intersarcomere Stiffness

The effect of removing intersarcomere stiffness can be seen by comparing Fig. 5 with Fig. 4 *A*. The initial rise is similar, the peak tension is not significantly different, but

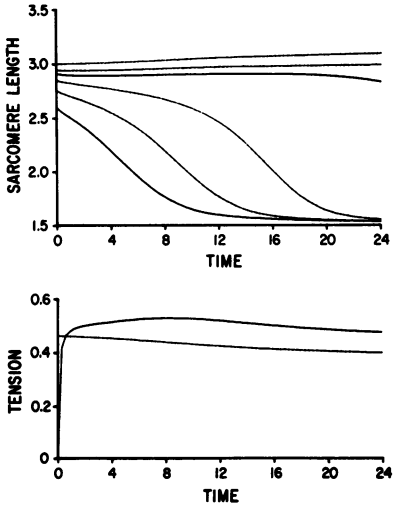

FIGURE 6 The more uniform fiber. The initial conditions were identical to Fig. 4 *A* except that the shortest sarcomere is now 2.75 μm instead of 2.6 μm. The creep is slower, but the peak force is greater.

the decline after the peak is greater, with the enhancement over the isometric capability decreasing. This is accompanied in the sarcomere length traces by the development of two sharply separated populations of sarcomeres with different lengths (some crossover occurs as the tension declines), rather than the smooth distribution, continuous incorporation of neighboring sarcomeres, and continued motion seen in Fig. 4 *A*. At the end of a long tetanus without intersarcomere stiffness, there are two sharply separated populations of sarcomeres, each with the same isometric capability but on opposite sides of the length-tension diagram, no transition zone, no movement and no enhancement of force, except by virtue of the passive length tension curve. Microscopy of living fibers and records of the length of a central segment of a fiber obtained with a spot follower apparatus, Fig. 4 *B*, agree with Fig. 4 *A* in showing a smooth transition and continued motion.

Degree of Non-uniformity

Experiments with successive tetani (Julian and Morgan 1979 *a*, Fig. 8) suggested that a more uniform fiber, while showing a slower creep phase, could in fact generate a greater peak tension than a less uniform (previously stimulated at long length) fiber. Comparison of Fig. 6 with Fig. 4 *A* shows that the model gives the same result. The initial range of sarcomere lengths is less, the rate of tension creep is less, and the peak occurs later, but the number of shortening sarcomeres is greater, as is the peak tension reached. Simulation runs with various initial distributions showed that the primary effect was on the rate of rise of the creep tension. Making the shortest sarcomeres shorter increased the rate of creep, while changing the length constant of the initial distribution had more complex but smaller effects, interacting with the intersarcomere stiffness.

DISCUSSION

The sarcomere model used here is very simple, being designed to fit the isometric sarcomere length-tension relationship, the force-velocity relationship, the passive tension curve, and the series elasticity of a real muscle fiber, and to include the concept of intersarcomere stiffness. It ignores the viscoelasticity of passive tension, and the complexities of sarcomere skewing and thick filament misalignment, and could not accurately simulate the slow decay of tension after a stretch applied during a contraction at optimal length, nor the slight dependence of a muscle force-velocity curve on the extent of movement. Despite this, and in agreement with real fibers, as shown in Figs. 3 *B* and 4 *B*, it showed the following phenomena. (*a*) Sarcomere lengths are unstable in a fiber stretched beyond the plateau, in that initial non-uniformities increase during activation. (*b*) These instabilities are heavily damped, leading to a slow stretching of central sarcomeres at rates up to 1% V_{max}, and relatively rapid shortening of small patches (<5% of fiber length) of initially slightly shorter sarcomeres at the ends. (*c*) This movement causes a slow increase in tension to a peak followed by a slow decline. (The time to peak in the model for a reasonable amount of non-uniformity corresponds to that seen in fibers within the variation seen from fiber to fiber and contraction to contraction, e.g., Julian and Morgan, 1979 *a*, Fig. 8.) (*d*) The transition between the region of shortened sarcomeres and the rest of the fiber is not abrupt, provided intersarcomere stiffness is included in the case of the model. There is a maintained transition region of sarcomeres with intermediate lengths, and hence isometric capabilities greater than the existing tension. (*e*) The motion and the tension enhancement above the isometric capability of the central sarcomeres continue throughout the tetanus by continuous incorporation of neighboring sarcomeres into the shortening regions. In the model, maintenance of this transition zone depends on the intersarcomere force. (*f*) Decreasing the initial non-uniformity of the fiber caused a slower "creep," but increased the peak tension produced, rather than decreasing it (Julian and Morgan 1979 *a*, Fig. 8). This casts serious doubt on the value of choosing fibers with smaller amounts of non-uniformity in an effort to reduce the effects of such non-uniformity, particularly the size of the creep phase of tension rise (ter Keurs et al., 1978). It is clear that the fast upstroke is more nearly equal to the isometric capability in Fig. 6 than Fig. 4 *A*, though always slightly higher so that the extrapolation technique of Gordon et al. (1966 *a*, Fig. 3) will be more accurate for a more uniform fiber or fiber segment. These authors of course controlled the length of a highly uniform central segment, which showed a very slow development of creep tension, and hence a highly accurate extrapolation. Moderately short tetani were used, with the result that the peak of tension was never reached for these very uniform segments (see Julian and Morgan 1979 *b* for a discussion of the difficulties involved in long duration segment length clamped tetani). This finding that extrapolation still overestimates tension but is more accurate when the creep is slower is in agreement with experiment. Extrapolation certainly provides a better estimate of isometric tension than does the peak tension, as the fiber is most uniform at the beginning of the tetanus.

On the other hand, the rate of fall of tension after the peak is significantly greater in the model than in experimental records. The unrealistically fast decay of tension after a stretch shown by the model sarcomere and the neglecting of velocity dependent passive tension could explain part of this, but it seems likely that other mechanisms omitted from the model may also contribute. In particular, the skewing of sarcomeres can also give rise to extra tension. Consider for example the situation shown in Fig. 7 *A* where Z-lines Z_1 and Z_3 are considered fixed and perpendicular to the fiber, but Z_2 is skewed. The situation is unstable, and the angle of Z_2 will increase, sarcomere S_1

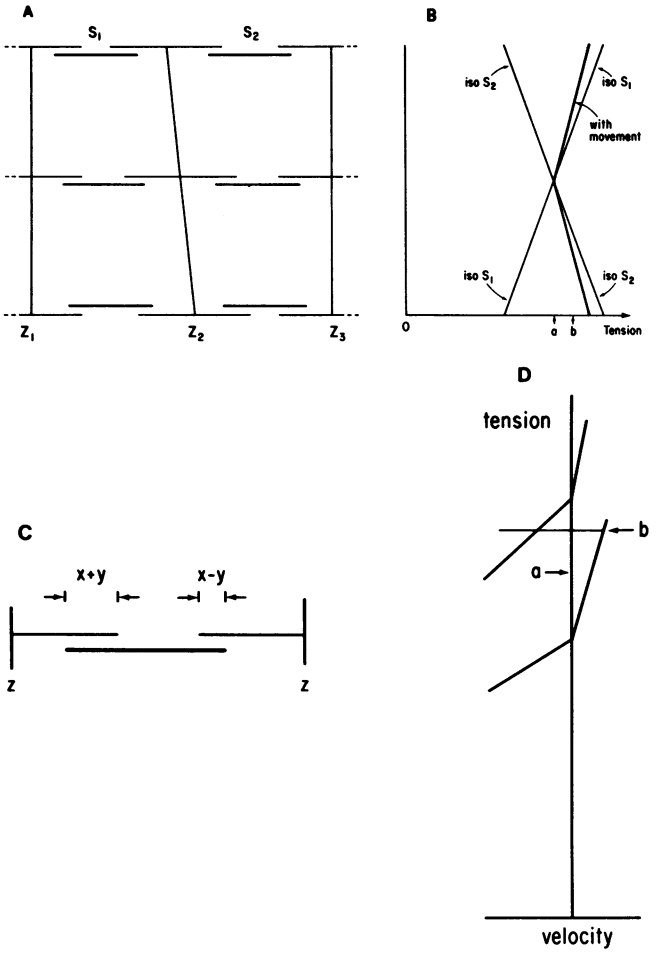

FIGURE 7 Other internal motion. *A*, the hypothetical situation of one skewed Z line, Z_2 between two sarcomeres S_1 and S_2. *B*, the variation of tension across the fiber. The ordinate represents position across the fiber for both *A* and *B*. The actual tension (thicker line) is the weighted sum of the isometric tensions of the two series sarcomeres, weighted according to the slopes of the force velocity curve (1:6). The tension appropriate to a sarcomere with the mean length (i.e., half Z_1 to Z_3) is shown by *a*, the actual tension with movement, averaged across the fiber, is shown by *b*. The amount of skew is exaggerated for clarity. *C*, displaced thick filaments are analogous to two unequal sarcomeres. If the original overlap was x, and the thick filaments are displaced by y, then force-velocity curves may be drawn for each half sarcomere, with isometric forces proportional to overlap and unloaded shortening velocities equal. For small velocities, the force velocity relationships may each be approximated by two straight lines as in *D*. If the overall sarcomere length is constant, the velocities of the two halves must be equal and opposite, i.e. *b* is the tension generated compared to *a* if the thick filaments were centred. For y small compared to x, the tension is that appropriate to an isometric sarcomere with overlap $x + 5/7\ y$. This is approximately true up to $y = 0.3x$, when give occurs in the shorter half.

shortening and S_2 lengthening at the top of the diagram, and vice versa at the bottom. The non-linearity of the force-velocity relationship means that the tension in each fibril across the fiber as in Fig. 7 *B* is greater than or equal to the isometric capability of a sarcomere with the mean length; i.e., sarcomere length equal to half the distance from Z_1 to Z_3.

Displacement of thick filaments (Fig. 7 *C*) similarly can generate extra tension, again because of the instability, internal motion, and non-linearity of the force-velocity curve. The initial non-uniformity (skew of sarcomeres, displacement of thick filaments) for these mechanisms would probably be much smaller than the sarcomere non-uniformity, (though they may be accentuated by movement) leading to a much slower development of extra tension, probably never developing to a peak in a contraction of realistic duration. As shown in Fig. 6, slower development does not mean less tension. This slow rise would add to the rise, peak and slow fall of the intersarcomere dynamics to give the total fiber response. Quantification of these effects would require electron microscopy of fibers fixed while actively contracting, for which techniques are now under development (Brown and Hill, 1979.)

It is concluded then that a simple model of intersarcomere dynamics using a lumped model of a sarcomere can simulate the main features of tension creep in fixed end contractions, but that other types of internal motion may also be significant. This supports the idea that the creep phase of tension rise is due to internal movement, further justifying the methods used by Gordon et al. (1966 *b*) to obtain their length-tension relationship.

We would like to acknowledge the cooperation of Dr. T. McMahon of Harvard University.

This work was supported by the following grants: an National Institutes of Health research grant, HL-16606, from the National Heart, Lung and Blood Institute, and grants from the American Heart Association, No. 77-616, and the Muscular Dystrophy Association.

Received for publication 5 February 1981 and in revised form 25 February 1982.

REFERENCES

Blinks, J. R. 1965. Influence of osmotic strength on cross-section and volume of isolated single muscle fibers. *J. Physiol.* (*Lond.*). 177:42–57.

Brown, L. M., and L. M. Hill. 1979. A new technique for the rapid fixation of skeletal muscle. *J. Physiol.* (*Lond.*). 289:8–9.

Edman, K. A. P. 1966. The relation between length and active tension in isolated semitendinosus fibres of the frog. *J. Physiol.* (*Lond.*). 183:407–417.

Edman, K. A. P. 1979. The velocity of unloaded shortening and its relation to sarcomere length and isometric force in vertebrate muscle fibres. *J. Physiol.* (*Lond.*). 291:143–159.

Fabiato, A., and F. Fabiato. 1978. Myofilament generated tension oscillations during partial calcium activation and activation dependence of the sarcomere length tension relation of skinned cardiac cells. *J. Gen. Physiol.* 72:667–699.

Ford, L. E., A. F. Huxley, and R. M. Simmons. 1977. Tension responses to sudden length change in stimulated frog muscle fibers near slack length. *J. Physiol.* (*Lond.*). 269:441–515.

Gordon, A. M., A. F. Huxley, and F. J. Julian. 1966 *a*. Tension development in highly stretched vertebrate muscle fibers. *J. Physiol.* (*Lond.*). 184:143–169.

Gordon, A. M., A. F. Huxley, and F. J. Julian. 1966 *b*. The variation in isometric tension with sarcomere length in vertebrate muscle fibres. *J. Physiol.* (*Lond.*). 184:170–192.

Haskell, R. C., and F. D. Carlson. 1981. Quasi-elastic light-scattering studies of single skeletal muscle fibers. *Biophys. J.* 33:39–62.

Hill, A. V. 1938. The heat of shortening and the dynamic constants of muscle. *Proc. Roy. Soc. B.* 126:136–195.

Huxley, A. F. 1980. Reflections on Muscle. Liverpool University Press.

Huxley, A. F., and L. D. Peachey. 1961. The maximum length for contraction in vertebrate striated muscle. *J. Physiol. (Lond.).* 165:150–163.

Huxley, A. F., and R. M. Simmons. 1970. A quick phase in the series-elastic component of striated muscle, demonstrated in isolated fibers from the frog. *J. Physiol. (Lond.).* 208:52–53p.

Huxley, A. F., and R. M. Simmons. 1971. Mechanical properties of the cross-bridges of frog striated muscle. *J. Physiol. (Lond.).* 218:59–60.

Julian, F. J., and D. L. Morgan. 1979 *a*. Intersarcomere dynamics during fixed-end tetanic contractions of frog muscle fibers. *J. Physiol. (Lond.).* 293:365–378.

Julian, F. J., and D. L. Morgan. 1979 *b*. The effect on tension of non-uniform distribution of length changes applied to frog muscle fibers. *J. Physiol. (Lond.).* 293:379–392.

Julian, F. J., R. L. Moss, and M. R. Sollins. 1978. The mechanism for vertebrate striated muscle contraction. *Circ. Res.* 42:2–14.

Julian, F. J., M. R. Sollins, and R. L. Moss. 1978. Sarcomere length non-uniformity in relation to tetanic responses of stretched skeletal muscle fibers. *Proc. Roy. Soc. Lond. B. Biol. Soc.* 200:109–116.

Katz, B. 1939. The relation between force and speed in muscular contraction. *J. Physiol. (Lond.).* 96:45–64.

Peachey, L. D., and B. R. Eisenberg. 1978. Helicoids in the T system and striations of frog skeletal muscle fibers seen by high voltage electron microscopy. *Biophys. J.* 22:145–154.

Ramsey, R. W., and S. F. Street. 1940. The isometric length tension diagram of isolated skeletal muscle fibers of the frog. *J. Cell. Comp. Physiol.* 14:11–34.

Rudel, R., and F. Zite-Ferenczy. 1979. Do laser diffraction studies on striated muscle indicate stepwise sarcomere shortening? *Nature (Lond.).* 278:573–575.

ter Keurs, H. E. D. J., T. Iwazumi, and G. H. Pollack. 1978. The sarcomere length-tension relation in skeletal muscle. *J. Gen. Physiol.* 72:565–592.